Scanning Near-Field Fluorescence Resonance Energy Transfer Microscopy

Sarah A. Vickery and Robert C. Dunn
Department of Chemistry, University of Kansas, Malott Hall, Lawrence, Kansas 66045

ABSTRACT A new microscopic technique is demonstrated that combines attributes from both near-field scanning optical microscopy (NSOM) and fluorescence resonance energy transfer (FRET). The method relies on attaching the acceptor dye of a FRET pair to the end of a near-field fiber optic probe. Light exiting the NSOM probe, which is nonresonant with the acceptor dye, excites the donor dye introduced into a sample. As the tip approaches the sample containing the donor dye, energy transfer from the excited donor to the tip-bound acceptor produces a red-shifted fluorescence. By monitoring this red-shifted acceptor emission, a dramatic reduction in the sample volume probed by the uncoated NSOM tip is observed. This technique is demonstrated by imaging the fluorescence from a multilayer film created using the Langmuir–Blodgett (LB) technique. The film consists of L-α-dipalmitoylphosphatidylcholine (DPPC) monolayers containing the donor dye, fluorescein, separated by a spacer group of three arachidic acid layers. A DPPC monolayer containing the acceptor dye, rhodamine, was also transferred onto an NSOM tip using the LB technique. Using this modified probe, fluorescence images of the multilayer film reveal distinct differences between images collected monitoring either the donor or acceptor emission. The latter results from energy transfer from the sample to the NSOM probe. This method is shown to provide enhanced depth sensitivity in fluorescence measurements, which may be particularly informative in studies on thick specimens such as cells. The technique also provides a mechanism for obtaining high spatial resolution without the need for a metal coating around the NSOM probe and should work equally well with nonwaveguide probes such as atomic force microscopy tips. This may lead to dramatically improved spatial resolution in fluorescence imaging.

INTRODUCTION

Fluorescence resonance energy transfer (FRET) proves to be an increasingly important technique for measuring proximity relations in proteins, nucleic acids, and membranes (Chen and Lentz, 1997; Dos Remedios and Moens, 1995; Gonzalez and Tsien, 1995; Miyawaki et al., 1997; Stryer, 1978; Van Der Meer et al., 1994). The method takes advantage of the strong distance dependence of nonradiative energy transfer from an excited donor molecule to an unexcited acceptor molecule. This dipole–dipole interaction, first described by Förster in 1948, has an inverse sixth power dependence on the intermolecular separation, making it sensitive to angstrom scale distance variations (Lakowicz, 1983; Stryer, 1978; Van Der Meer et al., 1994). The rate of energy transfer, k_T, between donor and acceptor is given by

$$k_t = \tau_d^{-1}(R_o/p)^6,$$

where τ_d is the unperturbed lifetime of the donor, r is the donor–acceptor separation, and R_o, the Förster distance, is the separation at which energy transfer is 50% efficient (Lakowicz, 1983; Van Der Meer et al., 1994). The last term contains components that account for the spectral overlap between the donor emission and acceptor absorption and an orientation factor, κ^2, that considers the relative spatial orientation of the two transition dipoles. The distance over which energy transfer is significant occurs on the tens of angstroms scale, ideal for monitoring dynamic processes in proteins or events occurring in or across biological membranes. This "spectroscopic ruler" has thus been exploited to monitor voltage changes in single cells, protein conformational motions, and in ion-sensing applications (Chen and Lentz, 1997; Dos Remedios and Moens, 1995; Gonzalez and Tsien, 1995; Miyawaki et al., 1997; Stryer, 1978; Van Der Meer et al., 1994).

Here, we report a new technique that combines FRET measurements with near-field scanning optical microscopy (NSOM). NSOM is an imaging technique that provides subwavelength optical resolution by scanning a small light source within nanometers of a sample surface (Betzig et al., 1991; Paesler et al., 1996; Pohl, 1991). The light source is usually fashioned from a single mode optical fiber that is heated and drawn to a fine point and then coated with aluminum around the sides to confine the light (Betzig et al., 1991). By positioning the probe within nanometers of the sample surface, optical measurements can be made with 50- to 100-nm spatial resolution. Such measurements have been applied to the study of single molecules (Ambrose et al., 1994; Betzig and Chichester, 1993; Trautman et al., 1994; Xie and Dunn, 1994), thin films (Higgins and Barbara, 1995; Higgins et al., 1996; Hollars and Dunn, 1997; Hollars and Dunn, 1998; Reid et al., 1996; Weston and Buratto, 1997), solid state systems (Grober et al., 1994; Hess et al., 1994; Hsu et al., 1996), and biological systems (Betzig et al., 1993; Dunn et al., 1994; Enderle et al., 1997). Several reports have also appeared in which FRET measurements

Received for publication 6 October 1998 and in final form 21 December 1998.

Address reprint requests to Robert C. Dunn, Department of Chemistry, University of Kansas, Malott Hall, Lawrence, KS 66045. Tel.: 785-864-4313; Fax: 785-864-5396; E-mail: rdunn@caco3.chem.ukans.edu.

© 1999 by the Biophysical Society

0006-3495/99/04/1812/07 $2.00

have been combined with the high resolution of NSOM (Brunner et al., 1997; Ha et al., 1996; Kerimo et al., 1998).

In this paper, we discuss a variation on the NSOM technique that incorporates the FRET mechanism to increase imaging capabilities (Sekatskii and Letokhov, 1996). The idea is shown schematically in Fig. 1. In this technique, an acceptor dye is attached to an NSOM probe that has not been coated with a metal. Light exiting the NSOM probe (*blue arrow*) is resonant with the donor dye in the sample but not the acceptor dye attached to the tip. As the NSOM tip approaches the sample surface, energy transfer can occur between the excited donor dye in the sample and the acceptor dye bound to the tip (*dark green arrow*). This coupling gives rise to a red-shifted fluorescence (*red arrow*) that can be selectively monitored using filters to block the donor dye emission (*light green arrows*).

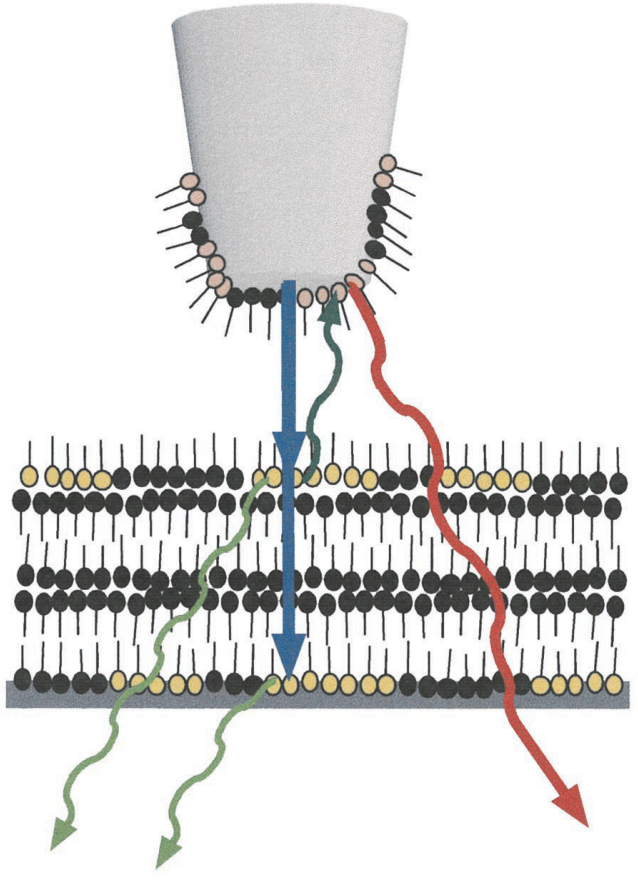

FIGURE 1 Schematic of the tip and sample configuration used in the FRET/NSOM experiments. The acceptor dye in the FRET pair, rhodamine, is incorporated into a DPPC monolayer at 0.5 mol% and attached to an NSOM probe that has not been coated with a metal. The donor dye in the sample, fluorescein, is incorporated into two DPPC/0.5 mol% fluorescein layers separated by a spacer of three arachidic acid layers. Light exiting the NSOM probe (*blue arrow*) is resonant with the donor dye in the sample but not with the acceptor dye attached to the tip. When the modified NSOM probe is near the sample, energy transfer from the excited donor to the rhodamine acceptor (*dark green arrow*) on the tip leads to a new emission to the red (*red arrow*) of the donor emission (*light green arrows*). By monitoring the red-shifted acceptor fluorescence, it is possible to optically probe only those structures located in closest proximity to the NSOM tip.

There are several advantages to using the FRET/NSOM configuration shown in Fig. 1. The novel coupling of microscopic techniques makes it possible to optically probe only those structures located closest to the NSOM tip. The strong distance dependence of FRET effectively reduces the interaction region between the tip and sample to that of closest approach. Therefore, NSOM probes do not have to be coated with an opaque metal such as aluminum to obtain subdiffraction limit spatial resolution. This increased z sensitivity may also lead to new ways of noninvasively monitoring small height changes in reduced sample regions. Moreover, because the technique does not require the formation of a small light source, it can be extended to other nonoptical probes such as atomic force microscopy (AFM) tips. This may result in a new generation of probes capable of much higher spatial resolution in fluorescence imaging than that currently attainable with conventional fiber optic NSOM probes. Finally, because the acceptor dye attached to the tip is nonresonant with the excitation light exiting the tip, photobleaching is dramatically reduced, leading to an increased probe lifetime.

In this paper, we demonstrate the feasibility of FRET/NSOM using multilayered lipid LB films doped with a donor dye. The use of dye infused into lipid films was chosen to provide a well defined system in which the chromophore location can be precisely controlled. The LB technique is also shown to provide a convenient method for transferring a highly controlled lipid monolayer incorporating an acceptor dye onto an uncoated NSOM tip. Fluorescence images of the multilayer film taken with a modified NSOM tip show features indicative of energy transfer from the sample to the tip. These results are discussed in the context of future experiments on thick samples, such as cells, and for very high resolution optical imaging using modified AFM probes.

MATERIALS AND METHODS

DPPC (Sigma), 5-octadecanoylaminofluorescein (Molecular Probes), octadecyl rhodamine B chloride (Molecular Probes), and arachidic acid (Aldrich Chemical) were used without further purification. DPPC and arachidic acid were dissolved in spectral grade chloroform to a concentration of 1 mg/mL. Concentrated solutions of fluorescein and rhodamine in ethanol and methanol, respectively, were added to the DPPC stock solution to yield samples of DPPC/0.50 mol% fluorescein and DPPC/0.50 mol% rhodamine. The lipid mixtures were dispersed onto an aqueous subphase and compressed using a computer-controlled LB trough (Nima Technology, Model 611) equipped with a Wilhelmy pressure sensor. The compression rate was 100 cm^2/min, and the films were transferred onto cleaned glass surfaces at a dipping velocity of 25 mm/min. Bilayers were transferred onto the glass surface in the liquid-condensed (LC)/liquid-expanded (LE) region (9 mN/m) using the LB technique for the first monolayer and the Langmuir–Schaefer technique to transfer the second layer (Gaines, 1966). For the multilayer films used in the FRET/NSOM experiments, all layers were transferred onto glass using the LB technique. The initial DPPC/0.50 mol% fluorescein layer was transferred onto the coverslip at a dipping velocity of 15 mm/min and a surface pressure of 14 mN/m. Three layers of arachidic acid were then transferred onto the substrate at a surface pressure of 25 mN/m followed by another DPPC/0.50 mol% fluorescein layer at 14 mN/m. DPPC/0.50 mol% rhodamine monolayers were trans-

ferred onto uncoated NSOM probes at a pressure of 6 mN/m, where the film is predominantly in the LE phase. Films were deposited at this relatively low position on the pressure isotherm to ensure maximum fluorophore coverage around the end of the tip.

The details of the microscope used to collect the images have been reported previously (Talley et al., 1998; Talley et al., 1996). Briefly, the microscope consists of a modified Bioscope atomic force microscope (Digital Instruments) mounted on an inverted fluorescence microscope (Zeiss Axiovert 135TV) equipped with a Zeiss fluar 40× (1.3 NA) oil immersion objective lens. The same microscope is capable of both confocal and near-field measurements. For NSOM imaging, the near-field tip is held in a custom designed shear-force head. For both confocal and NSOM measurements, the sample is scanned using a separate x-y closed-loop piezo scanner (Physik Instrumente). Excitation at 458 nm is provided by an argon ion laser (Liconix 5000) and at 543 nm by a 2 mW green helium neon laser (Particle Measuring Systems). The fluorescence generated by the sample and the tip is collected from below using the high NA objective lens, filtered using either a 548 nm (±5 nm) (Melles Griot) or a 590 nm (±5 nm) (Melles Griot) bandpass filter, and imaged onto an avalanche photodiode detector (EG&G, SPCM-200). The piezo scanning and data acquisition are controlled by a Digital Instruments Nanoscope IIIa control station and software.

RESULTS AND DISCUSSION

To implement the FRET/NSOM scheme, the well known donor–acceptor FRET pair of fluorescein and rhodamine, respectively, was used. As the schematic shown in Fig. 1 illustrates, the technique relies on attaching the rhodamine acceptor to the end of an NSOM tip and incorporating the fluorescein donor into the sample. In an effort to control the tip and sample geometry as much as possible, both fluorescent derivatives were incorporated into LB films of DPPC.

To provide a starting place for understanding the issues involved in FRET/NSOM and to optimize the energy transfer conditions, confocal fluorescence images were collected of a DPPC bilayer containing both FRET chromophores. The donor, fluorescein, was doped into DPPC at 0.5 mol% and transferred onto a clean glass coverslip using the LB technique. A second monolayer of DPPC containing 0.5 mol% of the rhodamine acceptor was transferred onto the first layer using the Langmuir–Schaefer technique as described previously (Gaines, 1966; Hollars and Dunn, 1998). Both monolayers were transferred at a surface pressure of 9 mN/m in the LC-LE phase coexistence region of DPPC (Cadenhead et al., 1980). In this region of the pressure isotherm, DPPC monolayers consist of fluorescent LE regions containing distinctive dark LC domains that exclude the fluorescent probe (Lösche et al., 1983; McConnell et al., 1984; Möhwald, 1990).

Figure 2 *A* shows a 23 × 23 μm confocal image of the bilayer fluorescence at 548 nm (±5 nm) following excitation at 458 nm. Excitation at 458 nm predominantly excites the fluorescein dye, and the bandpass filter, at 548 nm, excludes the rhodamine emission. Using this configuration provides an image in which the fluorescein-doped DPPC layer is preferentially probed. As expected, this side of the bilayer exhibits dark LC domains surrounded by LE regions containing the fluorescent dye. Alternatively, the other side of the bilayer, doped with the rhodamine dye, can be exclusively viewed by changing the excitation and emission wavelengths. Figure 2 *B* shows the confocal fluorescence image at 590 nm (±5 nm) of the same region of the bilayer following excitation at 543 nm. At these emission and excitation wavelengths, the DPPC/rhodamine layer is observed. The phase patterns observed in Fig. 2 *B* are markedly different from those shown in Fig. 2 *A*, illustrating that each side of the bilayer can be selectively probed. Finally,

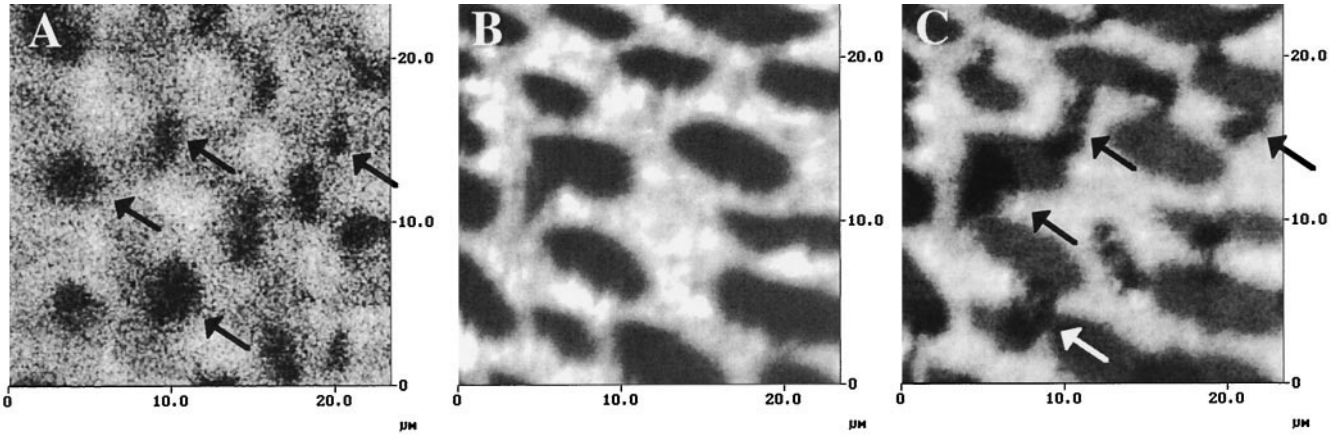

FIGURE 2 Far-field confocal fluorescence images of a DPPC bilayer in which the bottom monolayer contains 0.5 mol% fluorescein and the top layer contains 0.5 mol% rhodamine. (*A*) A 23 [mult] 23 μm image of bilayer fluorescence at 548 nm (±5 nm) following excitation at 458 nm. At these excitation and emission wavelengths, the fluorescence from the fluorescein layer is preferentially probed. The bright and dark areas of the film reflect the partitioning of the DPPC into the LE and LC phases, respectively. (*B*) Confocal fluorescence image of the same region of the film exciting at 543 nm and detecting at 590 nm (±5 nm). At these wavelengths, the upper layer of the film containing the rhodamine dye is probed. As in (*A*), the LE-LC phase partitioning in the film is readily apparent. (*C*) Confocal fluorescence image after combining excitation at 458 nm, which excites the fluorescein in the bottom layer, and detecting at 590 nm, which passes the rhodamine emission from the upper layer. Rhodamine fluorescence is observed only in areas of the bilayer where dye-doped LE regions from each side of the bilayer overlap, and energy transfer can occur. New dark regions appear in the image (*arrows*) where LC regions from the fluorescein layer are located.

by combining excitation at 458 nm, which excites the fluorescein dye, and filtering the collected fluorescence through the 590-nm bandpass filter, which passes the rhodamine emission, energy transfer from the bottom DPPC layer to the top of the bilayer can be imaged. This is shown in Fig. 2 *C* for the same bilayer region. In this image, rhodamine fluorescence is only observed from regions of the bilayer in which the dye containing LE domains on each side of the bilayer overlap, and energy transfer can take place. In regions of the bilayer where there are dark LC regions in the bottom fluorescein-doped layer, energy transfer to the upper rhodamine/DPPC layer does not occur, and new dark regions are observed in the fluorescence image. Several of these regions are indicated by the arrows in Figs. 2 *A* and *C*.

These images demonstrate the ability to discriminate between fluorescein and rhodamine fluorescence induced by direct excitation and rhodamine emission arising from energy transfer from the fluorescein layer. The fluorescence image shown in Fig. 2 *C* also indicates that energy transfer between the two sides of the bilayer occurs with high efficiency. This is evidenced by the low intensity, quenched fluorescein fluorescence (Fig. 2 *A*) and the strong energy transfer rhodamine emission (Fig. 2 *C*). Efficient energy transfer is also evidenced by the large contrast observed for the new dark features in Fig. 2 *C*. These observations are consistent with the close proximity of the chromophores in the bilayer and the R_o of 55 Å for this FRET pair (Van Der Meer et al., 1994).

To illustrate the feasibility of FRET/NSOM, a test sample was constructed of DPPC/0.5 mol% fluorescein layers separated by a spacer consisting of three arachidic acid layers. This is shown schematically in Fig. 1. The arachidic acid spacers provide a gap between the two fluorescein-doped layers, making energy transfer from the upper DPPC/fluorescein layer to the NSOM probe much more favorable than that from the bottom layer. The DPPC/0.5 mol% fluorescein films were transferred onto the glass substrate at a higher surface pressure than that used in the films shown in Fig. 2 to increase their stability and to decrease decomposition of the film during the multilayer deposition process.

The LB technique was also used to attach a monolayer containing the acceptor dye, rhodamine, to the end of an uncoated NSOM probe. This was done to precisely control the thickness of the dye-containing film and to limit the range of κ^2 (the orientation factor) in the Förster distance term (Dos Remedios and Moens, 1995; Stryer, 1978; Van Der Meer et al., 1994). To demonstrate that a well-defined monolayer can be transferred onto a tip using this technique, Figs. 3 *A* and *B* show fluorescence images of modified probes. The images present side views of probes that have been coated with DPPC/0.5 mol% rhodamine at 9 mN/m and 6 mN/m, respectively. As before, the monolayer on the probe shown in Fig. 3 *A*, coated at 9 mN/m, exhibits distinctive dark and bright regions. This pattern is indicative of coexisting LC and LE lipid phases and confirms the presence of a complete monolayer. The film on the probe shown in Fig. 3 *B* was deposited at a lower surface pressure where DPPC is predominantly in the LE phase. At this pressure, the fluorescence coverage at the end of the NSOM probe is highly homogeneous, reducing the possibility that a nonfluorescent LC domain will coat the very end of the tip. For the FRET/NSOM experiments to be discussed, all NSOM probes were coated at this pressure.

For FRET experiments, it is important that the monolayer be intact around the end of the NSOM tip. This proves difficult to address directly given the dimensions of the tips shown in Figs. 3 *A* and *B*. To investigate whether the films

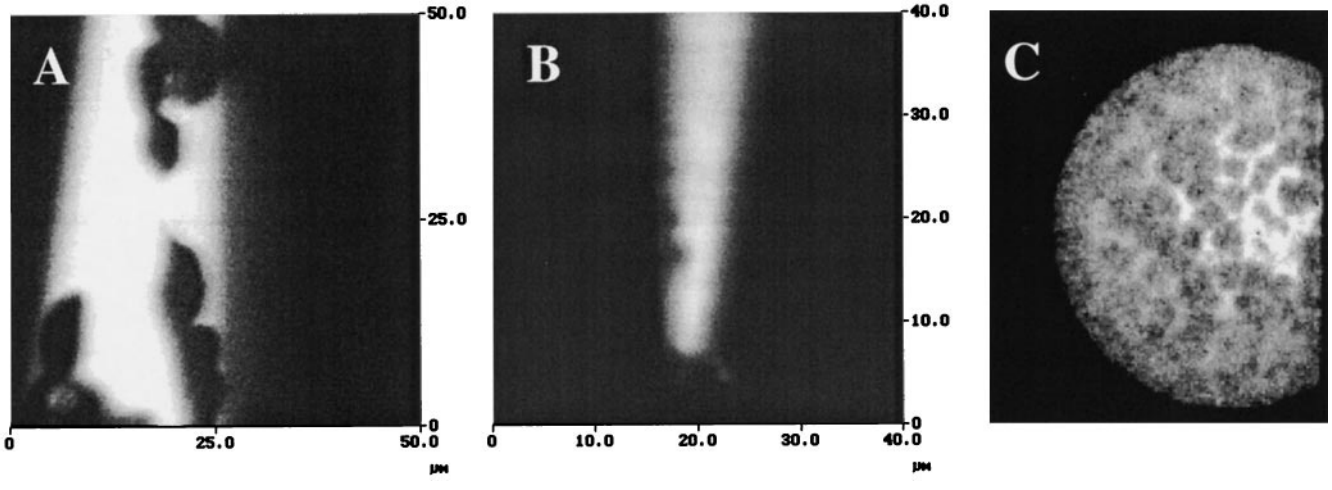

FIGURE 3 Confocal fluorescence images of DPPC/0.5 mol% rhodamine modified NSOM probes coated at (*A*) 9 mN/m and (*B*) 6 mN/m. The tip coated in (*A*) exhibits the distinctive LC-LE phase partitioning indicating that a complete monolayer is transferred onto the NSOM tip. The monolayer coated onto the tip in (*B*) exists mainly in the LE phase producing a more homogenous coverage of the fluorescent rhodamine. All FRET/NSOM probes used in experiments were coated at this pressure. (*C*) Fluorescence image of the end of a cleaved fiber (125 μm diameter) coated with a DPPC/rhodamine monolayer at 9 mN/m. The phase patterns show that a monolayer can be coated around corners, which provides evidence that similar monolayers uniformly coat the apex of the NSOM probes.

can completely cover the aperture of the tip, a monolayer was transferred onto the end of a cleaved fiber at a pressure of 9 mN/m. Figure 3 *C* displays a fluorescence image of the very end of the cleaved fiber, which exhibits the distinctive LC-LE phase patterns. Even around the sharp corners of a cleaved fiber, the monolayer remains intact and the phase patterns are unaltered. It is likely, therefore, that, for the pulled NSOM probes shown in Figs. 3 *A* and *B*, the LB film is able to form a complete monolayer around the apex of the tip. Together, the fluorescence images in Fig. 3 illustrate the ability to transfer a well-defined monolayer onto an uncoated NSOM probe with the LB technique.

To investigate the feasibility of FRET/NSOM, LB-coated NSOM probes were used to fluorescently image the multilayer films of DPPC/fluorescein and arachidic acid. Two experimental conditions are compared to investigate the energy transfer to the NSOM probe and the resulting effect on imaging capabilities. Figure 4 *A* shows a 50 $\times$ 50 μm NSOM fluorescence image at 548 nm of the multilayer film following excitation at 458 nm. As shown earlier in the far-field confocal measurements, 458 nm preferentially excites the fluorescein dye, and the 548 nm bandpass filter selectively passes the fluorescein emission. This arrangement, therefore, is sensitive to the fluorescein emission from the sample. The image contains fluorescently doped LE domains that are smaller and more random than those observed in Fig. 2, consistent with the higher surface pressure used in transferring this film. It is not possible from Fig. 4 *A* to discern which fluorescent domains are in the uppermost or bottom DPPC layers of the film.

This image can be compared with the fluorescence image shown in Fig. 4 *B* taken in the same sample area. Figure 4 *B* was collected with the 590 nm filter such that the rhodamine fluorescence from the DPPC-coated tip was monitored. For this image, the excitation wavelength of 458 nm remained the same, thus exciting the fluorescein in the sample. Fluorescence contrast is therefore reflective of energy transfer from the excited fluorescein in the sample to the rhodamine attached to the end of the NSOM tip. There exists a striking difference between the fluorescence features observed in Figs. 4 *A* and *B*, which are exemplified by the circled region and the features marked by arrows. The arrows denote bright fluorescent LE domains in Fig. 4 *A* that are dramatically less intense in Fig. 4 *B*. Alternating between the two imaging modes proves that these differences are not simply the result of photobleaching or other nonreversible processes. As the sample is scanned under the tip, only those fluorescein-containing domains in the uppermost monolayer of the sample can efficiently transfer their energy to the modified NSOM probe. This leads to diminished intensity for the domains marked by arrows that are farther from the modified NSOM tip and enhanced fluorescence for domains in the uppermost layer of the film.

There is also a noticeable increase in the fluorescence resolution seen in Fig. 4 *B* as compared to Fig. 4 *A*, even though both images were collected using the same tip. This, again, is a manifestation of the energy transfer process and can be observed by examining the circled region of each image. It is not surprising that the resolution observed in Fig. 4 *A* is poor because the NSOM tip used in the imaging did not have a metal coating. Normally, these coatings are required to form the small aperture on the NSOM tip enabling high resolution imaging. However, in the FRET/NSOM image shown in Fig. 4 *B*, the strong distance dependence in the FRET signal leads to energy transfer only from areas of the sample and tip that are within closest proximity

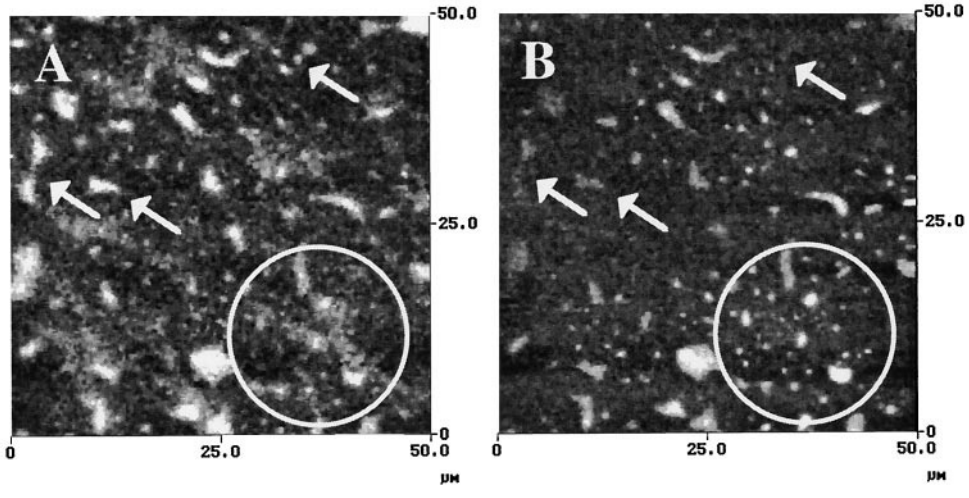

FIGURE 4 NSOM fluorescence images, 50 [mult] 50 μm, of the multilayer film schematically shown in Fig. 1. (*A*) NSOM fluorescence image at 548 nm following excitation at 458 nm. As shown in Fig. 3, these excitation and detection wavelengths are sensitive to the fluorescein emission and should not contain energy transfer contributions from the rhodamine-coated tip. The fluorescent domains in both of the DPPC/fluorescein layers contribute to the structure seen in this image. (*B*) FRET/NSOM fluorescence image taken by monitoring the rhodamine emission at 590 nm and exciting the fluorescein sample at 458 nm. This image contains fewer fluorescent domains, demonstrating the increased discrimination between the two sides of the film. Examples of these areas are marked by arrows. The r^{-6} distance dependence in FRET also leads to increased spatial resolution in the FRET/NSOM image. This can be seen by comparing the circled regions in each image.

to each other. This leads to a new mechanism for obtaining high spatial resolution, which can be seen by comparing the circled regions of Figs. 4 *A* and *B*. To further illustrate the resolution enhancement in FRET/NSOM, Fig. 5 shows an 11 × 11 μm image of the same sample. In this image, fluorescent features arising from energy transfer between the sample and the modified NSOM probe lead to features with half-widths of approximately 140 nm. This is roughly the size of the NSOM tip and demonstrates the selective probing enabled by the strong distance dependence of the FRET signal.

It is intriguing to consider the number of applications that can be implemented using this new technique. The most obvious is the possibility of carrying out fluorescence measurements with much higher spatial resolution than currently possible. The FRET technique discussed here does not rely on the formation of a small light source as does NSOM. This removes many of the obstacles currently blocking progress in pushing the resolution limit in these measurements. For instance, the technique introduced here should work equally well with nonwaveguide tips such as AFM probes. By attaching an acceptor dye to the end of an AFM tip and using far-field excitation to excite a donor dye in a sample, much higher optical resolution in FRET imaging should be attainable. The technique may also offer a new way for probing small sample motions in a noninvasive manner. By positioning the modified probe over a region of interest containing a donor dye, small changes in the tip sample gap will lead to large changes in the energy transfer efficiency. Finally, combining FRET with NSOM may also lead to a reduction in the sample volume probed with NSOM as illustrated in Fig. 4. For thick samples such as cells, this reduction in probe volume may lead to new insights into membrane organization and may even be useful in studying the asymmetry between the cytoplasmic and extracellular membrane faces.

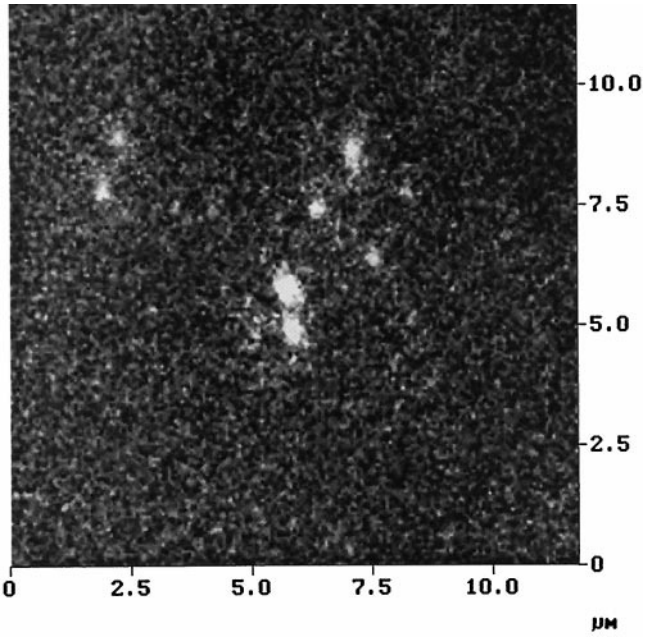

FIGURE 5 An 11 [mult] 11 μm FRET/NSOM fluorescence image of the same sample shown in Fig. 4. High resolution fluorescent features with half-widths of approximately 140 nm are observed even though the image was taken with an NSOM tip not coated with a metal to confine the light. The high resolution results from the strong distance dependence in the FRET signal and demonstrates the possibility of high resolution optical imaging with nonwaveguide probes such as AFM tips.

CONCLUSIONS

A novel microscopic technique is reported that combines characteristics from NSOM and FRET to provide a new method for probing samples with high spatial resolution. The goals of combining the strong distance dependence of FRET with the NSOM technique include a reduction in the probe volume in NSOM for applications on thick samples such as cells, an increase in the *z* sensitivity for single point dynamic measurements, a simplification of NSOM probe fabrication by eliminating the need for the metal coating, and the introduction of a scheme that can be extended to nonwaveguide-type probes such as AFM tips. The last example is a straightforward extension of the measurements demonstrated here and should dramatically improve the spatial resolution in fluorescence microscopy. These capabilities provide new ways of probing the fluorescent properties of samples with both high lateral and axial resolution and should offer new insights into sample structures at the nanometric scale.

S.A.V. gratefully acknowledges support from the University of Kansas–Madison and Lila Self Graduate Fellowship. Support for this work was provided by National Science Foundation (NSF) grant number CHE-9612730, NSF-CAREE grant no. CHE-9703009, and the Searle Scholars Program/The Chicago Community Trust.

REFERENCES

Ambrose, W. P., P. M. Goodwin, J. C. Martin, and R. A. Keller. 1994. Alterations of single molecule fluorescence lifetimes in near-field optical microscopy. *Science*. 265:364–367.

Betzig, E., and R. J. Chichester. 1993. Single molecules observed by near-field scanning optical microscopy. *Science*. 262:1422–1425.

Betzig, E., R. J. Chichester, F. Lanni, and D. L. Taylor. 1993. Near-field fluorescence imaging of cytoskeletal actin. *Bioimaging*. 1:129–135.

Betzig, E., J. K. Trautman, T. D. Harris, J. S. Weiner, and R. L. Kostelak. 1991. Breaking the diffraction barrier: optical microscopy on a nanometric scale. *Science*. 251:1468–1470.

Brunner, R., A. Bietsch, O. Hollricher, O. Marti, and A. Lambacher. 1997. Application of a near-field optical microscope to investigate the fluorescence energy transfer between chromophores embedded in Langmuir–Blodgett films. *Surf. Inter. Anal.* 25:492–495.

Cadenhead, D. A., F. Müller-Landau, and B. M. J. Kellner. 1980. Phase transitions in insoluble one and two-component films at the air/water interface. *In* Ordering in Two Dimensions, S. K. Sinha, editor. Elsevier, Amsterdam, The Netherlands. 73–81.

Chen, Q., and B. R. Lentz. 1997. Fluorescence resonance energy transfer study of shape changes in membrane-bound bovine prothrombin and Meizothrombin. *Biochemistry*. 36:4701–4711.

Dos Remedios, C. G., and P. D. J. Moens. 1995. Fluorescence resonance energy transfer spectroscopy is a reliable "ruler" for measuring structural changes in proteins. *J. Struct. Biol.* 115:175–185.

Dunn, R. C., G. H. Holtom, L. Mets, and X. S. Xie. 1994. Near-field fluorescence imaging and fluorescence lifetime measurements of light harvesting complexes in intact photosynthetic membranes. *J. Phys. Chem.* 98:3094–3098.

Enderle, T., T. Ha, D. F. Ogletree, D. S. Chemla, C. Magowan, and S. Weiss. 1997. Membrane specific mapping and colocalization of malarial and host skeletal proteins in the *Plasmodium falciparum* infected erythrocyte by dual-color near-field scanning optical microscopy. *Proc. Natl. Acad. Sci. USA*. 94:520–525.

Gaines, G. L. 1966. Insoluble Monolayers at Gas Liquid Interfaces. Interscience, New York.

Gonzalez, J. E., and R. Y. Tsien. 1995. Voltage sensing by fluorescence resonance energy transfer in single cells. *Biophys. J.* 69:1272–1280.

Grober, R. D., T. D. Harris, J. K. Trautman, E. Betzig, W. Wegscheider, L. Pfeiffer, and K. West. 1994. Optical spectroscopy of a GaAs/AlGaAs quantum wire structure using near-field scanning optical microscopy. *Appl. Phys. Lett.* 64:1421–1423.

Ha, T., T. Enderle, D. F. Ogletree, D. S. Chemla, P. R. Selvin, and S. Weiss. 1996. Probing the interaction between two single molecules: fluorescence resonance energy transfer between a single donor and a single acceptor. *Proc. Natl. Acad. Sci. USA*. 93:6264–6268.

Hess, H. F., E. Betzig, T. D. Harris, L. N. Pfeiffer, and K. W. West. 1994. Near-field spectroscopy of the quantum constituents of a luminescent system. *Science*. 264:1740–1745.

Higgins, D. A., and P. F. Barbara. 1995. Excitonic transitions in J-aggregates probed by near-field scanning optical microscopy. *J. Phys. Chem.* 99:3–7.

Higgins, D. A., P. J. Reid, and P. F. Barbara. 1996. Structure and exciton dynamics in J-aggregates studied by polarization-dependent near-field scanning optical microscopy. *J. Phys. Chem.* 100:1174–1180.

Hollars, C. W., and R. C. Dunn. 1997. Submicron fluorescence, topology and compliance measurements of phase separated lipid monolayers using tapping-mode near-field scanning optical microscopy. *J. Phys. Chem.* 101:6313–6317.

Hollars, C. W., and R. C. Dunn. 1998. Submicron structure in L-α-dipalmitoylphosphatidylcholine monolayers and bilayers probed with confocal, atomic force, and near-field microscopy. *Biophys. J.* 75: 342–353.

Hsu, J. W. P., E. A. Fitzgerald, Y. H. Xie, and P. J. Silverman. 1996. Studies of electrically active defects in relaxed GeSi films using a near-field scanning optical microscope. *J. Appl. Phys.* 79:7743–7749.

Kerimo, J., D. M. Adams, P. F. Barbara, D. M. Kaschak, and T. E. Mallouk. 1998. NSOM investigations of the spectroscopy and morphology of self-assembled multilayered thin films. *J. Phys. Chem. B*. 102: 9451–9460.

Lakowicz, J. R. 1983. Principles of Fluorescence Spectroscopy. Plenum Press, New York.

Lösche, M., E. Sackmann, and H. Möhwald. 1983. A fluorescence microscopic study concerning the phase diagram of phospholipids. *Ber. Bunsenges. Phys. Chem.* 87:848–852.

McConnell, H. M., L. K. Tamm, and R. M. Weis. 1984. Periodic structures in lipid monolayer phase transitions. *Proc. Natl. Acad. Sci. USA*. 81: 3249–3253.

Miyawaki, A., J. Llopis, R. Heim, J. M. McCaffery, J. A. Adams, M. Ikura, and R. Y. Tsien. 1997. Fluorescent indicators for Ca^{2+} based on green fluorescent proteins and calmodulin. *Nature*. 388:882–887.

Möhwald, H. 1990. Phospholipid and phospholipid-protein monolayers at the air/water interface. *Annu. Rev. Phys. Chem.* 41:441–476.

Paesler, M. A., and P. J. Moyer. 1996. Near-Field Optics: Theory, Instrumentation, and Applications. John Wiley and Sons, Inc., New York.

Pohl, D. W. 1991. Scanning near-field optical microscopy (SNOM). *In* Advances in Optical and Electron Microscopy, Vol. 12, T. Mulvey and C. J. R. Sheppard, editors. Academic Press, London, UK. 243–312.

Reid, P. J., D. A. Higgins, and P. F. Barbara. 1996. Environment-dependent photophysics of polymer-bound J aggregates determined by time-resolved fluorescence spectroscopy and time-resolved near-field scanning optical microscopy. *J. Phys. Chem.* 100:3892–3899.

Sekatskii, S. K., and V. S. Letokhov. 1996. Single fluorescence centers on the tips of crystal needles: first observation and prospects for application in scanning one-atom fluorescence microscopy. *Appl. Phys. B*. 63: 525–530.

Stryer, L. 1978. Fluorescence energy transfer as a spectroscopic ruler. *Ann. Rev. Biochem.* 47:819–846.

Talley, C., M. A. Lee, and R. C. Dunn. 1998. Single molecule detection and underwater fluorescence imaging with cantilevered near-field fiber optic probes. *Appl. Phys. Lett.* 72:2954–2956.

Talley, C. E., G. Cooksey, and R. C. Dunn. 1996. High resolution fluorescence imaging with cantilevered near-field fiber optic probes. *Appl. Phys. Lett.* 69:3809–3811.

Trautman, J. K., J. J. Macklin, L. E. Brus, and E. Betzig. 1994. Near-field spectroscopy of single molecules at room temperature. *Nature*. 369: 40–42.

Van Der Meer, B. W, G. Coker, and S.-Y. Simon Chen. 1994. Resonance Energy Transfer Theory and Data. VCH Publishers, Inc., New York.

Weston, K. D., and S. K. Buratto. 1997. A reflection near-field scanning optical microscope technique for subwavelength resolution imaging of thin organic films. *J. Phys. Chem. B* 101:5684–5691.

Xie, X. S., and R. C. Dunn. 1994. Probing single molecule dynamics. *Science*. 265:361–364.